Title Page

Characterizing and minimizing the contribution of sensory inputs to TMS-evoked potentials

Mana Biabani [a], Alex Fornito [a], Tuomas P. Mutanen [b], James Morrow [a], Nigel C. Rogasch [a]

[a] Brain and Mental Health Research Hub, Monash Institute of Cognitive and Clinical Neuroscience, School of Psychological Sciences, Monash Biomedical Imaging, Monash University, VIC, Australia

[b] Centre for Cognitive Neuroimaging, Institute of Neuroscience and Psychology, University of Glasgow, Glasgow G12 8QB, United Kingdom

Correspondence

Mana Biabani

Email : Mana.biabanimoghadam@monash.edu

Nigel C. Rogasch

Email : Nigel.rogasch@monash.edu

Address: Monash University, Building 220, Clayton Campus, 770 Blackburn Rd. Clayton, VIC, 3800, Australia

Abstract

Background: Transcranial magnetic stimulation (TMS) evokes voltage deflections in electroencephalographic (EEG) recordings, known as TMS-evoked potentials (TEPs), which are increasingly used to study brain dynamics. However, the extent to which TEPs reflect activity directly evoked by magnetic rather than sensory stimulation is unclear.

Objective: To characterize and minimize the contribution of sensory inputs to TEPs.

Methods: Twenty-four healthy participants received TMS over the motor cortex using two different intensities (subthreshold, supra-threshold) and waveforms (monophasic, biphasic). TMS was also applied over the shoulder as a multisensory control condition. Common sensory attenuation measures, including coil padding and noise masking, were adopted. We examined spatiotemporal relationships between the EEG responses to the scalp and shoulder stimulations at sensor and source levels. Furthermore, we compared three different filters (independent component analysis, signal-space projection with source-informed reconstruction (SSP-SIR) and linear regression) designed to attenuate the impact of sensory inputs on TEPs.

Results: The responses to the scalp and shoulder stimulations were correlated in both temporal and spatial domains, especially after ~60 ms, regardless of the intensity and stimuli waveform. However, the outputs of all filtering methods confirmed that TEPs cannot be entirely explained by sensory potentials. Among the three filters, SSP-SIR showed a good trade-off between preserving early TEPs, while correcting sensory-contaminated late components.

Conclusions: The findings demonstrate that motor TEPs reflect a combination of TMS-evoked and sensory-evoked neural activity, highlighting the importance of

adopting sensory control conditions in TMS-EEG studies. Offline filters show promise for isolating TMS-evoked neural activity from sensory-evoked potentials.

Keywords

TMS, TMS-evoked potential, sensory potential, control condition, offline filter

Highlights

- EEG responses to TMS over M1 (TEPs) and shoulder (SEPs) were compared
- Long latency components (> ~60ms) were correlated between TEPs and SEPs
- Changing TMS intensities and waveforms did not alter TEP-SEP relationships
- However, TEPs cannot be entirely explained by SEPs
- Offline filters showed promise for isolating TMS-evoked neural activity

Introduction

The combination of transcranial magnetic stimulation (TMS) and electroencephalography (EEG) has become an increasingly popular technique, since it has extended the application of TMS to study brain dynamics across the cortex [1, 2]. TMS-evoked potentials (TEPs) appear as voltage deflections in EEG recordings time-locked to the TMS pulse, which occur within a 300 to 500-ms long time window following stimulation, and can be used to make inferences about cortical reactivity and connectivity [1, 3, 4]. Recent studies have suggested that certain TEP peaks may reflect specific aspects of neurotransmission [5-7]. For instance, pharmacological evidence has shown that earlier TEP peaks following stimulation of motor cortex (e.g. N45) are sensitive to neurotransmission mediated by GABA-A receptors, whereas later peaks (e.g. N100) are sensitive to GABA-B receptor mediated activity [5, 7-9]. However, the mechanisms underlying many aspects of TEPs are still not perfectly understood [10, 11]. There is also debate over how much of the TEP signal represents direct activation of the cortex by TMS compared with other artefactual sources emanating from the recording equipment, blinks and muscle activity [12-15].

One potential confound of TEPs is the interaction of TMS with the sensory system [11, 12, 14, 15]. TMS is accompanied by a loud clicking noise, which results in auditory evoked potentials with peaks at similar intervals to TEPs, especially around N100 and P180. In addition, TMS activates sensory afferents in the underlying skin both mechanically by coil vibrations (e.g. a tapping sensation), and electrically by depolarizing the afferents fibers of cranial and facial nerves, which results in somatosensory-evoked potentials [13, 16]. These two types of sensory-evoked potentials (SEPs) are often minimized during the experiment by playing white noise to

mask the TMS click, and by using a layer of foam between the coil and scalp to dampen coil vibration [13, 17]. Although these methods are commonly assumed to render the distorting effects of SEPs negligible [13, 16, 18, 19], several recent studies have demonstrated similarities between TEPs following TMS and realistic control conditions (e.g. stimulation of the shoulder or electrical stimulation of scalp with a TMS click) despite the SEP-masking procedures [20-22]. These findings raise concerns regarding the specificity of TEPs to TMS-evoked cortical activity and underscore the urgent need for methods to further suppress sensory-evoked activity in TEP recordings.

There were two aims of the current study. The first aim was to characterize the contribution of sensory inputs to TEPs following stimulation of motor cortex. The second aim was to assess different offline methods for suppressing sensory responses in motor TEP recordings. We compared the efficacy of three different filtering methods in suppressing SEPs, as they have shown success in suppressing other types of artefacts such as ocular, decay and muscle artefacts [15, 23]. Finally, we repeated the above procedures by changing the intensity and waveform of the stimulations to examine the generality of the effects across different stimulation parameters.

Methods

Participants

Two separate experiments were conducted for this study. A total of 24 right-handed healthy individuals between the ages of 18 and 40 years were recruited. Twenty participants took part in experiment I (24.50 ± 4.86 years; 14 females) and 16

participants (25.82 ± 5.99 years; 11 females) participated in experiment II. Twelve individuals were common between experiments. All participants were screened for any contraindications to TMS [24], and provided their written consent prior to testing. All procedures were approved by the Monash University Human Ethics Committee in accordance with the declaration of Helsinki. Participants were seated comfortably with their elbows resting on the armrests, and their forearms pronated and rested on a pillow on their lap. They were also asked to keep their eyes open and focus on a black screen in front of them.

EMG

Electromyographic (EMG) activity was recorded from the right first dorsal interosseous (FDI) muscle, using bipolar surface Ag-AgCl electrodes (4-mm active diameter), placed in a belly-tendon montage with a distance of ~2 cm. The ground electrode was positioned on the dorsum of the right hand, over the midpoint of the third metacarpal bone (see supplementary methods for more details).

EEG

EEG recordings were made using a SynAmps^2 EEG system (Neuroscan, Compumedics, Australia), from 62 TMS-compatible Ag/AgCl-sintered ring electrodes, embedded in an elastic cap (EASYCAP, Germany). The electrodes were positioned according to the 10–20 international system, online-referenced to FCz and grounded to AFz. Electrode positions were co-registered to each subject's MRI by means of a neuronavigation system (Brainsight™ 2, Rogue Research Inc., Canada) and digitized (see supplementary methods for more details).

TMS

In experiment I, biphasic TMS pulses were applied to the hand area of left M1, where stimulation could induce consistent MEPs with greatest amplitude in FDI muscle [25], using a figure-of-eight coil (C-B60) connected to a MagPro X100+Option stimulator (MagVenture , Denmark). The neuronavigation system was used to guide TMS coil positioning and improve consistency across stimulation trials. Resting motor threshold (rMT) was determined as the minimum TMS intensity required to elicit MEPs >50 μV in at least 5 of 10 consecutive trials (with EEG cap on), and was expressed as a percentage of maximum stimulator output (% MSO)[26]. Each participant received 100 TMS pulses at an intensity of 120% rMT. As a control condition, 100 additional TMS pulses (120% rMT) were administered to participants' shoulder over the left acromioclavicular joint to mimic auditory and somatosensory sensations experienced during TMS. We changed the orientation and angle of the coil until the participants reported the same level of local sensations under the coil between the real TMS and control conditions. While this control condition does not perfectly match the scalp sensation of TMS, it does control for the general sensory experience of the stimulation. To investigate the effect of the stimulation intensity, each individual also received 100 TMS pulses with the intensity of 80% rMT over the left M1, in the same session. In experiment II, the effect of the waveform was explored by applying supra-threshold monophasic pulses over the left M1 and shoulder.

During both scalp and shoulder stimulation conditions, all of the currently advised measures to minimize multisensory inputs were implemented [19], including attaching a thin layer of foam underneath the coil to minimize coil vibration and bone-conducted auditory activation, and playing white noise through inserted earphones to minimize

air-conducted auditory activation. For each individual, the intensity of the white noise was increased until the click sound produced by the stimulations at 120% rMT was unperceivable or the sound pressure reached their upper limit of comfort. All of the participants reported that a small remnant of the acoustic clicks was still perceivable during the stimulation blocks, even when the volume was set to their upper threshold of comfort (see supplementary methods for more details).

EEG analysis

Analysis of EEG recordings was performed using custom scripts on the MATLAB platform (R2016b, The Mathworks, USA), EEGLAB [27], and TESA [28] toolboxes. The pipeline for cleaning and analyzing TMS-EEG data was based on the method described in [15, 28] (supplementary methods). Cortical sources of the evoked potentials were estimated using the Brainstorm (v3) software [29] and customized MATLAB scripts employing both minimum norm estimation (MNE) and dipole fitting methods (detailed in supplementary methods). All code for EEG processing and statistical analyses is available at https://github.com/BMHLab/TEPs-SEPs, and all clean data can be downloaded from https://figshare.com/s/d19e40ed1f02b8ada178. The raw data is also available upon request.

Suppression of SEPs

In order to suppress the contribution of SEPs from TEPs, we applied three different filtering techniques to each individual's responses: 1) linear regression; 2) independent component analysis (ICA); and 3) signal-space projection with source-informed reconstruction (SSP-SIR). Linear regression involved obtaining the line of the best fit between the SEPs (from the control condition) and TEPs (from the real

condition) at each point of time across electrodes, followed by subtracting the fitted SEP curves from the TEP data. For ICA, TEPs and SEPs from each individual were concatenated and submitted to the FastICA algorithm [30] (in addition to the two ICA steps already made in EEG pre-processing). SSP-SIR is a spatial filtering method, originally designed to remove TMS-evoked muscle artefacts [14]. We applied SSP-SIR to TEPs by following all the steps detailed in [14]. However, instead of using the frequency properties of muscle artefacts to estimate the projection matrix, we used the SEP data to estimate the artifactual dimensions to be removed from TEPs. To increase the accuracy, we applied the defined projection matrix to the lead-field matrix to take into account the distortions of the data in the inverse solution. For both ICA and SSP-SIR, we retained the *k* components that explained more than 90% of variance in SEP trials and removed those from the TEP data. In total, 8.6±4.17 and 12.3±2.34 components were rejected by ICA and SSP-SIR, respectively. (see supplementary for the topography of the rejected components by SSP-SIR).

A major issue in evaluating the success of artifact suppression methods is the lack of a ground truth (i.e. knowing what the TMS-evoked cortical activity should look like without SEP contamination). Therefore, we assessed the SEP suppression methods based on the assumption that the level of suppression should be related to the level of contamination (i.e. an ideal SEP suppression method should cause minimal distortion to TEPs when the relationship with SEPs is weak and vice versa). To test this assumption, we qualitatively compared TEPs before and after applying each filter at both scalp and source (estimations obtained using MNE) levels, and also measured their correlations across three different time windows. As a further assessment, we examined whether the quality of the source localization was altered using different filtering methods. Based on the assumption that short latency TEPs reflect localized

activities around the site of stimulation, we expected that reducing contamination would improve dipole fitting at the earliest time point (N20). We assessed the quality of the dipole fit using a goodness of fit (GOF) measure (supplementary methods), and also compared the distance between the best-fit dipole source found in pre- and post-suppressed data at N20.

Statistical analysis

All statistical analyses were performed in MATLAB. To compare the absolute values of TEPs and SEPs voltage levels across time and space, we applied cluster-based permutation tests over time and electrodes, as implemented in the FieldTrip toolbox [31]. To explore the relationships between the cortical responses to M1 and shoulder stimulations, we applied Spearman rank correlation tests across space (i.e. across electrodes at each time point) and time (i.e. across time for each electrode). Seven frequently studied peaks including N20, P30, N45, P60, N100, P180 and N280 were selected to examine the spatial correlations for each individual, and also to explore inter-individual variability in the TEP/SEP relationship. The spatial correlations were also examined for all points of time by testing the 95% of confidence intervals of correlation values against zero. The temporal correlations were assessed for each individual and each channel at three different time intervals (early, middle and late post-stimulus). To account for inter-individual variability in temporal properties of EEG responses, instead of defining fixed time windows for all subjects, the intervals were individualized according to the appearance of TEP peaks (i.e. N20-P60, P60-P180, P180-N280).

For group level analyses, the correlation results were transformed to z using Fisher's transform and statistical significance was assessed by applying one-sample permutation tests to test the null hypothesis that the individuals' z scores at each peak or time interval were equal to zero [32, 33]. The family-wise error rate due to multiple testings across time and channels was controlled for by adjusting the p-values using the t_{max} method proposed by Blair & Karniski [34]. The z scores were subsequently transformed back to the original scale for presentation. The results of source-localization (GOF-values and TMS-target-to-dipole-location distance) were compared between groups using paired-sample permutation tests with 10,000 shuffles.

Results

TEP-SEP comparisons

Fig. 1 illustrates the spatiotemporal distribution of grand-average TEPs and SEPs. All of the canonical TEP peaks were visible following M1 stimulation, with mean amplitudes ranging from ~-8 to +8μV (Fig. 1A). In contrast, SEPs showed smaller voltage deflections ranging from ~-4 to +4μV, with clear peaks at N100, P180 and N280, and only small peaks within the first 50 ms (Fig. 1B). Cluster-based permutation tests confirmed that TEPs were larger in amplitude than SEPs across time (Fig. 1C).

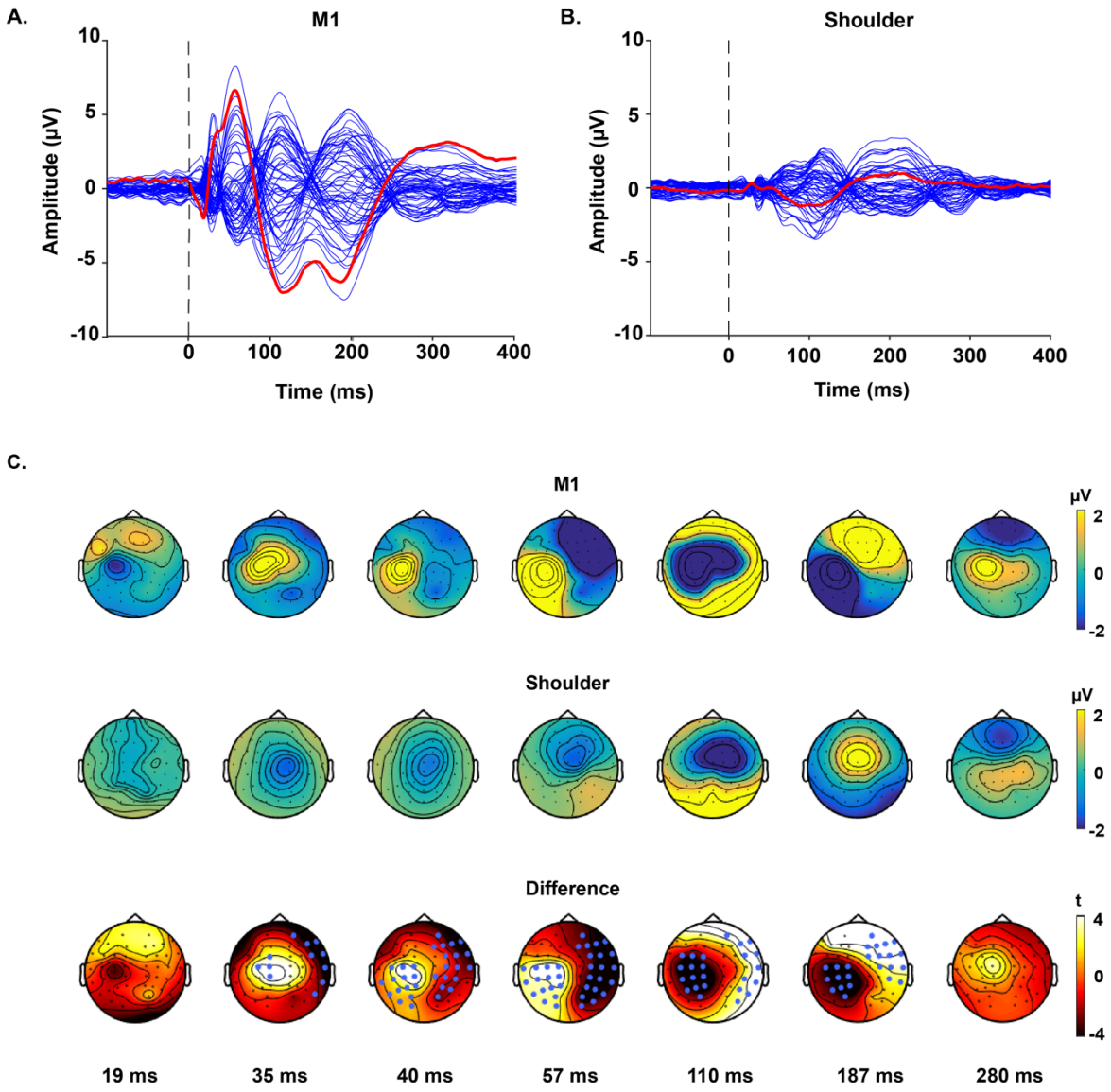

Fig. 1: TMS-evoked potentials following suprathreshold, biphasic stimulation over left M1 and left shoulder. The butterfly plots show the grand-average of potentials recorded by each electrode. A) Responses to the stimulation of M1. B) Responses to the stimulation of shoulder. The red line indicates the recordings by the electrode underneath the coil (C3). The vertical dash line at zero time point indicates the point of time when TMS is applied. C) The upper and middle topoplots depict voltage distributions across the scalp for each peak of interest, in response to the real and control conditions, respectively. The lower topoplots illustrate the results of the cluster-based permutation tests comparing the voltage distribution of the two responses at

each peak. Clusters were defined as at least two neighbouring electrodes exceeding the threshold of p-value < 0.05 at each point of time. Monte Carlo p-values were calculated on 5000 iterations with a critical α level set at p<0.025. The channels highlighted by blue dots belong to the clusters that showed statistically stronger responses to the real TMS condition. Two negative and three positive significant clusters were found.

Despite the amplitude differences between conditions, correlation analysis between spatial maps at each time point showed a consistent relationship (confidence intervals > 0) between TEPs and SEPs after ~60 ms (Fig. 2A), suggesting a common underlying source after this time. As the exact timing of TEP peaks differ between individuals, we repeated the analysis using individualised peak times (Fig. 2B). The correlations between TEPs and SEPs showed high inter-individual variability at the earlier peaks, whereas the majority of participants showed significantly positive correlations between the conditions for the N100, P180 and N280 peaks. Analyses of the temporal correlations further confirmed the strong relationships between SEPs and TEPs after 60 ms. As depicted in Fig. 2C, none of the electrodes showed significant correlation between time series between 20-60 ms. However, a large number of electrodes showed positive correlations between 60-180 ms (35 of 62) and 180-280 ms (25 of 62). Of note, correlation values were highest over a cluster of fronto-central electrodes associated with SEPs. The lowest correlation values were found over a cluster centred over the stimulation site (M1).

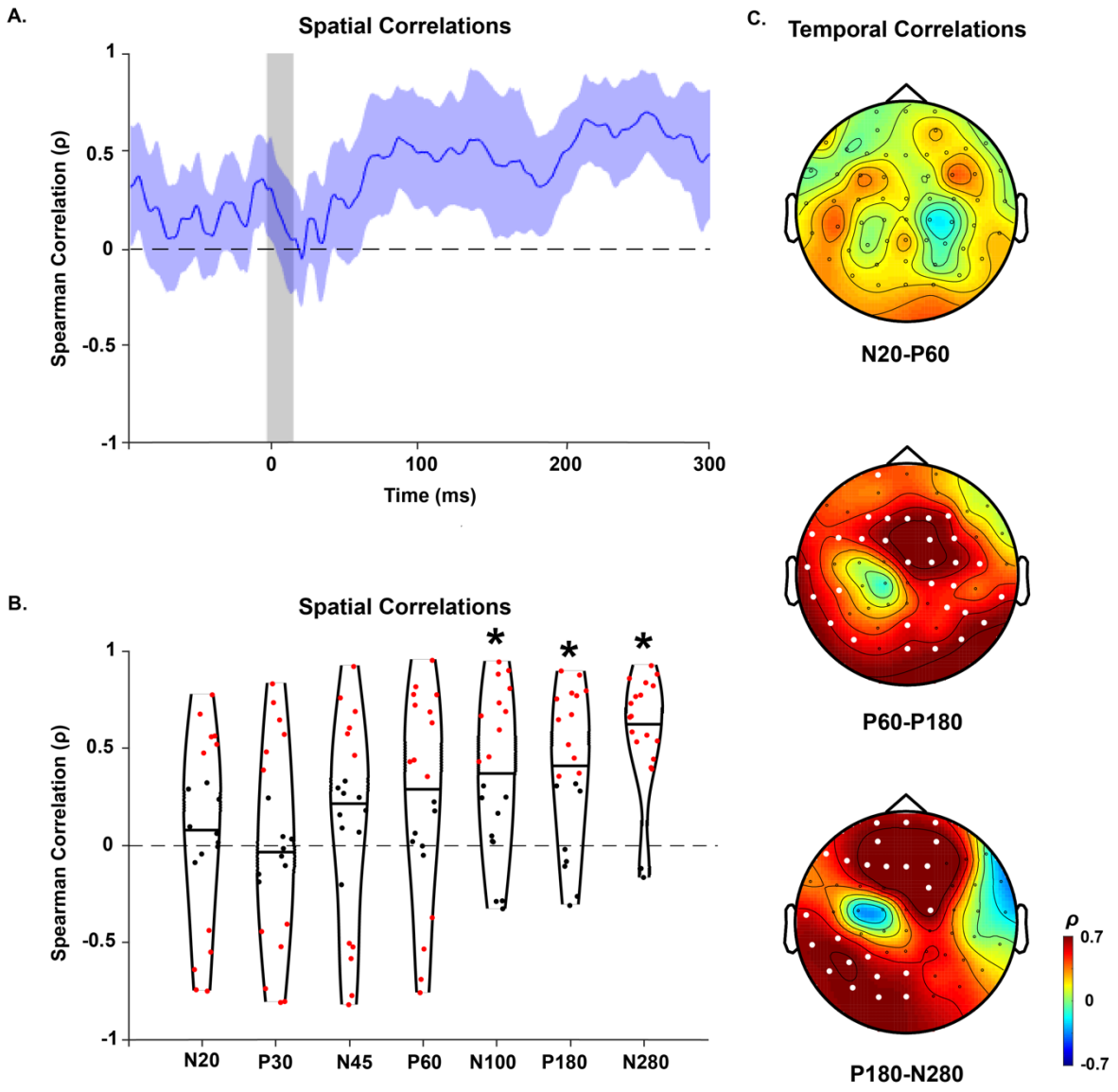

Fig. 2: Spatiotemporal correlations of TEPs and SEPs. A) Spatial correlations between TEPs and SEPs at each point of time from 100 ms before to 300 ms following stimulations. The blue shaded area represents the 95% confidence intervals. The vertical grey bar shows the window of interpolated potentials around stimulus. B) The distribution of spatial correlations across individuals at the time of individualised TEP peaks. The dots within the violin plots represent the correlation values for each individual. The red dots above and below the zero line show significant positive and negative correlations, respectively ($p<0.05$), and the black dots represent non-

significant correlations. * indicates that correlation values differed from 0 at the group level (one-sample t-test, $p<0.05$). C) The temporal correlations of the potentials at each window of time. White dots indicate the electrodes with significant positive correlations ($p<0.05$). No significant negative correlations were found.

Impacts of different SEP suppression methods on TEPs

Given that SEPs and TEPs showed high spatiotemporal correlation, we next compared three common methods for suppressing unwanted signals in TEP data: linear regression, ICA and SSP-SIR. Linear regression slightly diminished TEP amplitude, whereas, ICA exerted a strong impact on both temporal and spatial aspects of TEPs. The voltage range was considerably reduced and the peaks following 100 ms almost disappeared in C3 recordings. SSP-SIR preserved all the prominent peaks observed in the original data recorded by C3, but also caused a considerable reduction in voltage amplitude. The spatial maps of the SSP-SIR-filtered TEPs demonstrated a fairly consistent pattern across all of the examined peaks centering the largest potentials near the site of stimulation (Fig. 3).

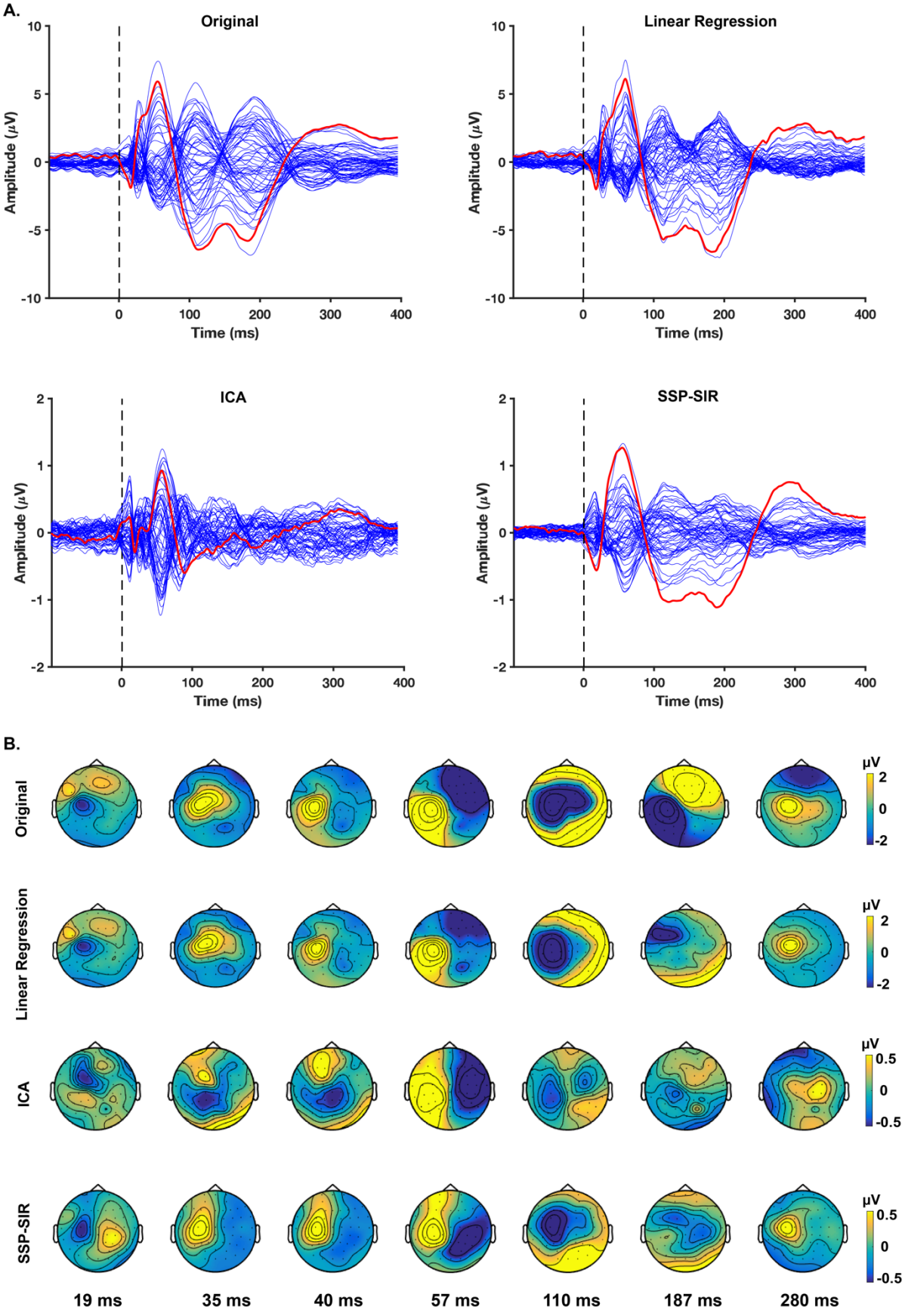

Fig. 3: The alterations in the spatiotemporal distributions of TEPs induced by

suprathreshold and biphasic TMS before and after removing SEPs using three different filtering methods. A) The butterfly plots demonstrate the grand-average of the potentials recorded by each electrode before (original) and after employing each filtering method. The red line indicates the recordings by the electrode underneath the coil (C3). The vertical dash line indicates the point of time when TMS is applied. B). The topoplots depict voltage distributions across the scalp for each peak of interest before (original) and after applying each filter.

To compare the impact of the filters on distributed source estimation, we applied MNE to the responses before and after TEP cleaning. Before filtering, the real TMS condition showed a focal cortical activity around the site of stimulation at N20, following which the estimated sources gradually scattered and spread across hemispheres, showing a similar distribution to the sources estimated following shoulder stimulation. As depicted in Fig.4 the three filtering methods changed the pattern of the estimated source differently, with SSP-SIR constraining source activity close to the site of stimulation. Since using the same threshold level across conditions and/or time points could have caused non-optimal maps for visual comparisons, we carried out quantitative assessments of the filter-induced alterations to TEPs. We measured the correlation between TEPs before and after applying each filter at three different windows of time, at both sensor (for each channel) and source (for each vertex) levels (Fig.5). At the scalp level, data following linear regression showed significant correlations with the original signal across all of time and space suggesting sub-optimal suppression of the sensory signal. A similar pattern was observed following ICA, although to a lesser extent at the later time window. SSP-SIR, however, resulted in low correlations (high suppression) especially around the fronto-central regions, which had shown high contamination. High

correlations (low suppression) were observed at the recordings around the site of stimulation where TEPs had shown minimum correlations with SEPs. Similar to the scalp level, SSP-SIR showed low correlation with the original signal at the source level.

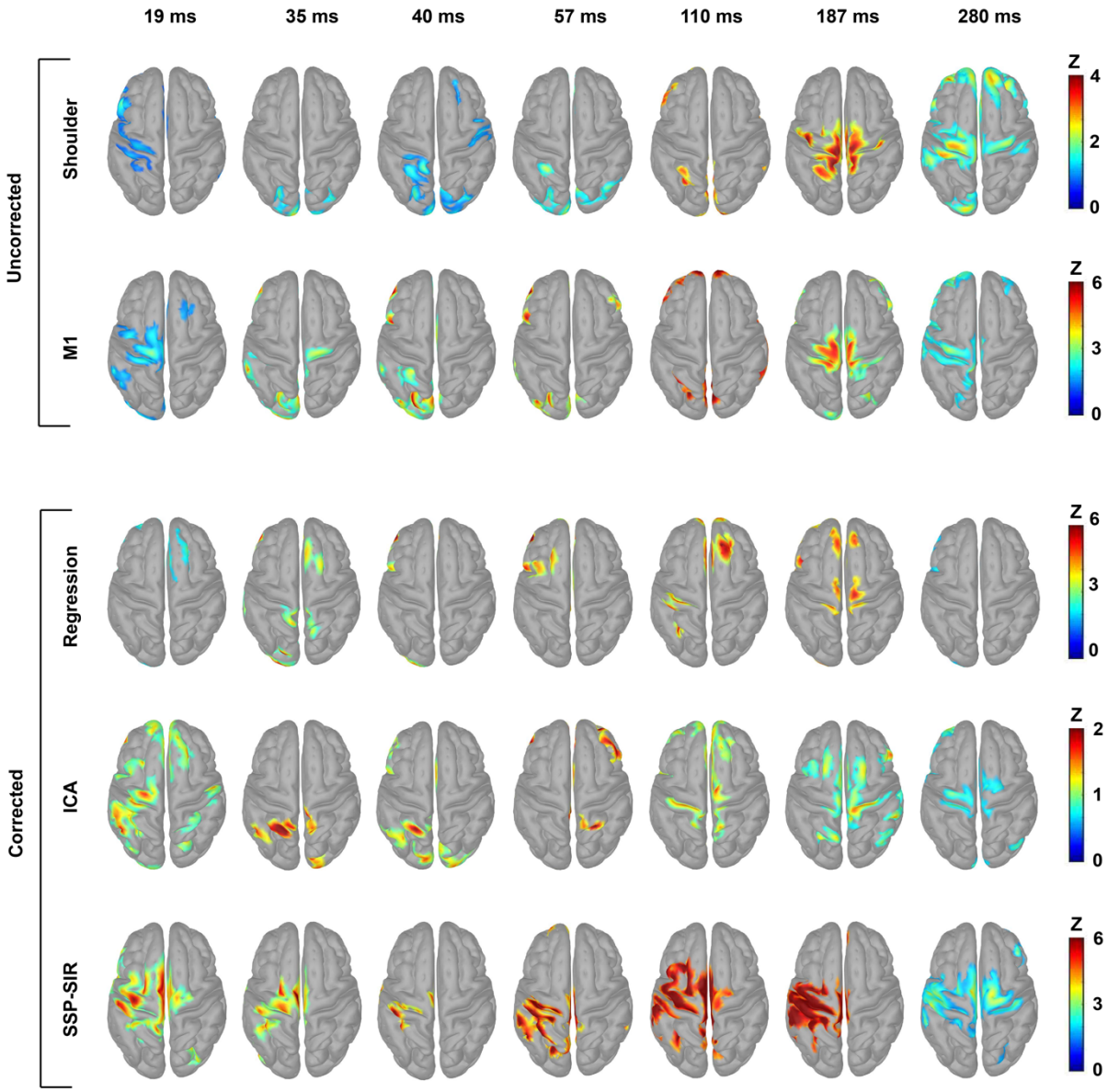

Fig. 4: The estimated source distributions obtained by applying MNE to the TEPs from different filtering methods. MNE maps are thresholded at 40% of the maximum activity at each point of time and the minimum size for the activated regions is set to 50 vertices (for Linear Regression the active regions at P180 were smaller than 50

vertices; therefore, the minimum size was decreased to 30). Linear-regression altered the pattern of the estimated sources at some time points, importantly, at 20 ms when no change was expected. However, the pattern of source activation remained similar to shoulder stimulation for the later time points (e.g. N100 and P180). For ICA, sources are largely contained to left and right somatomotor cortices, sharing similarities with SEPs at some timepoints (e.g P180, N280). The estimated sources from SSP-SIR filtered TEPs are predominantly centered around the area under stimulation, substantially different from the pattern observed following shoulder stimulation.

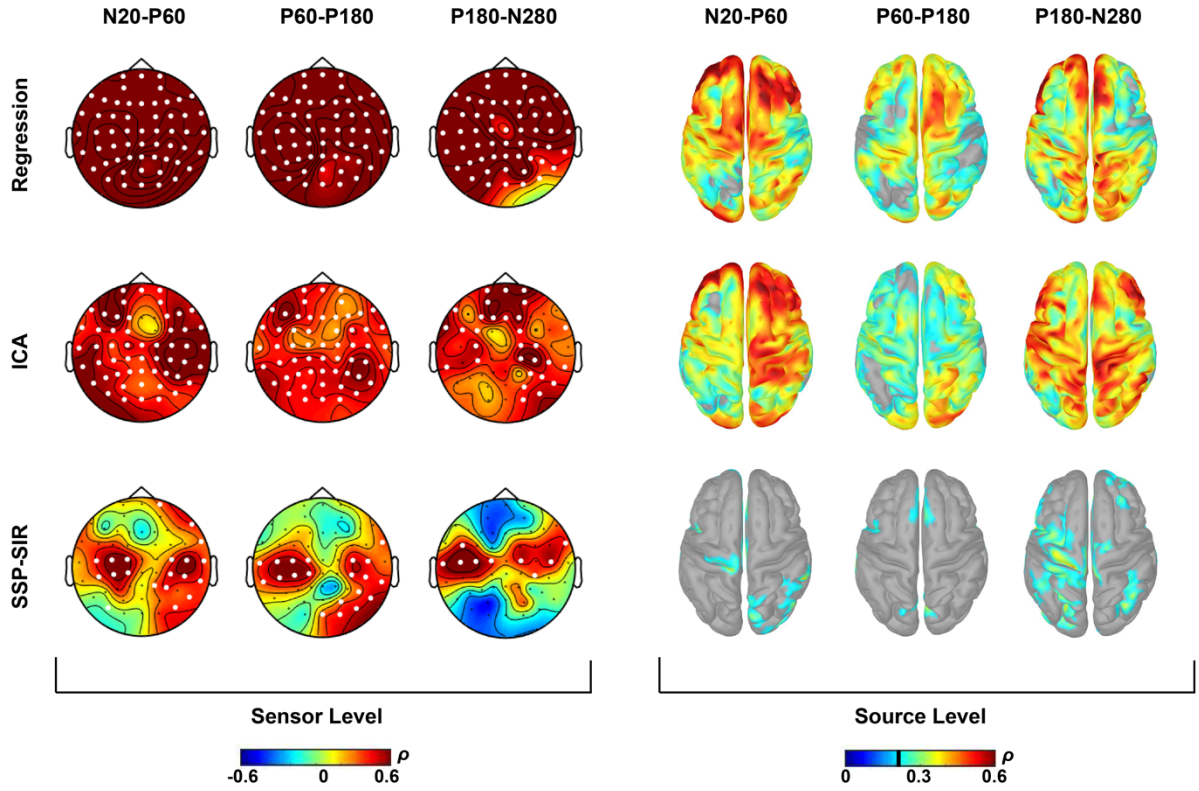

Fig. 5: Spearman correlation measures between the original and filtered TEPs at both sensor and source levels at three different intervals. The maps show the average of the correlation values at individualized time windows (i.e. N20-P60, P60-P180, P180-N280). A) The correlations between the original and filtered potentials recorded by each channel at each window of time. White dots indicate the electrodes with significant positive

correlations ($p<0.05$). B) The distribution of the correlations between the estimated source activities at each vertex. The source maps are thresholded at $\rho>0.2$.

To assess how each filtering method changed the quality of dipole fitting, we compared the best fit dipole found at N20 in the original and filtered data (Fig. 6). As depicted in Fig. 6, SSP-SIR substantially improved the GOF of TEP source estimations (permutation paired t-test with t_{max} correction, $p>0.05$), whereas the other filters reduced the GOF. All of the filtering methods resulted in significant displacement of the best fitting dipole (permutation paired-t test; $p<0.05$), while linear regression and ICA caused minimum and maximum repositions, respectively.

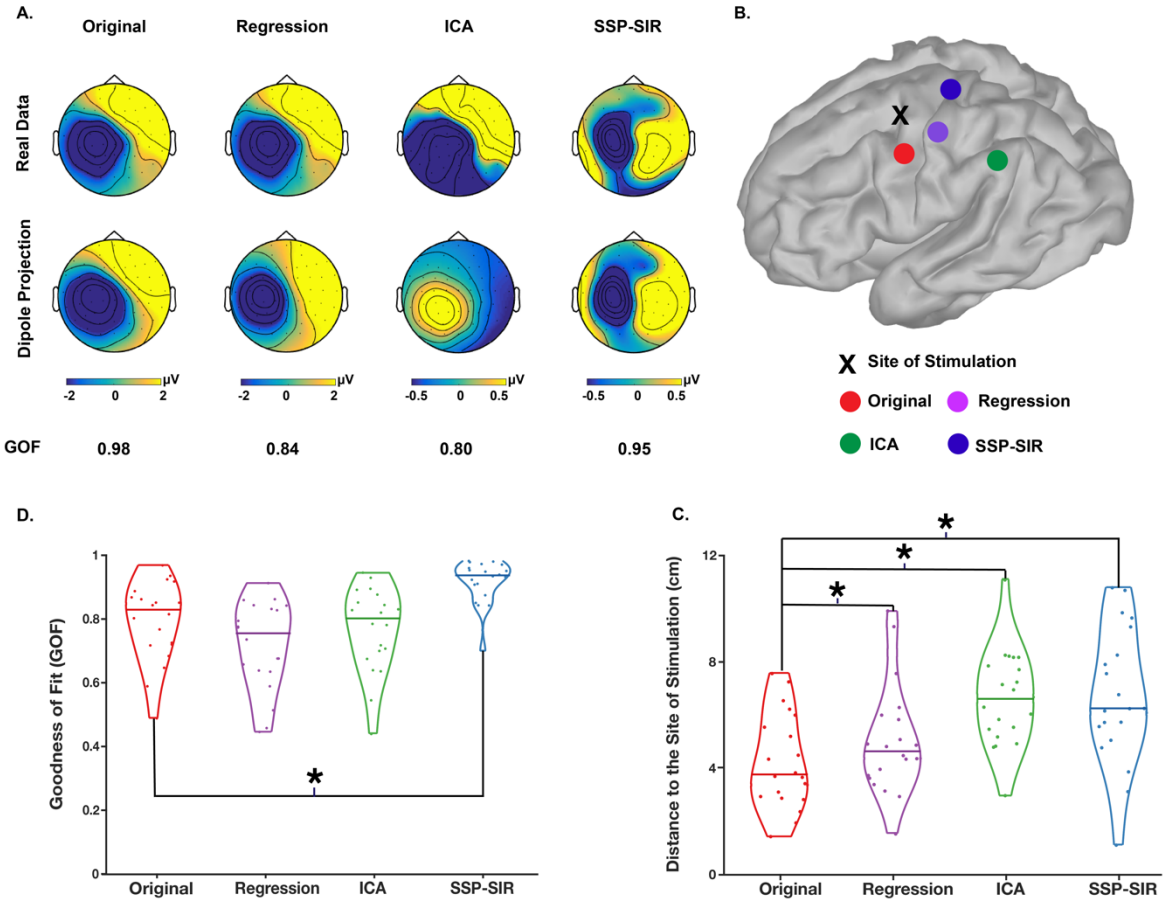

Fig. 6: Comparisons of the effects of the different filtering methods on source

localization at N20. A) Illustration of the measurements of goodness of fit (GOF), which represents the similarity between the topography of the real recorded data (upper plots) and the simulated responses produced by the dipole identified from each type of filtered data (lower plots), for one individual. B) Illustration of the measurements of the distances between the best-fit dipoles and the site of stimulation, for the same individual. C) Distribution of GOF for the best-fitting dipole source across individuals. * Indicates the significant change from raw data at the group level ($P<0.05$). D) Distance of the fitted dipole to the site of stimulation. The dots on violin plots represent the distance value for each individual. * Indicates the significant difference of the average distances between pre and post filtered potentials

Effect of stimulation parameters on TEP/SEP relationship and suppression

Decreasing the stimulation intensity substantially reduced the TEP amplitude relative to suprathreshold stimulation (to ~$\pm 2\mu V$) and changed the spatial distribution of voltages especially at the earlier peaks (i.e. N45 and P60; Supplementary, Fig. 1). Cluster-based permutation tests revealed significantly stronger responses to the control condition especially at central electrodes, following ~60 ms (supplementary Fig. 1). Spatiotemporal correlation tests showed that the TEPs evoked by subthreshold stimulations were highly correlated with SEPs evoked by suprashreshold pulses after about 45 ms, with more inter-individual consistency after 60 ms (Supplementary, Fig. 2). Despite the stronger responses to the control condition, SSP-SIR did not entirely suppress TEP peaks, especially at the earlier time points (<60ms), and the potentials remained significantly above baseline (baseline = 300 ms pre-stimulation, threshold = mean±3SD of baseline, $P<0.05$) (supplementary Fig. 3).

Changing to the monophasic simulation waveform did not alter the spatiotemporal distribution of cortical responses compared to biphasic stimulation (n=12; P>0.025, cluster-based permutation tests). Similar to the suprathreshold biphasic condition, responses to monophasic stimulation over M1 were stronger than those to shoulder stimulation; however, at the alpha level of 0.025 the significant clusters were only found at N100 and P180 (supplementary Fig. 4). In addition, SEPs and TEPs evoked by monophasic TMS followed very similar correlation patterns as observed in the responses to biphasic stimulations, in both spatial and temporal domains (supplementary Fig. 5). SSP-SIR substantially decreased the potential amplitudes to ~$\pm$1μV, preserving the original pattern of deflections and shifting the maximum amplitudes towards the site of stimulation at scalp and the majority of the peaks at source level, similar to the biphasic condition (supplementary Fig. 6 and 7).

Discussion

In the present study, we investigated the contributing effect of sensory inputs to TMS-evoked potentials and investigated different offline filtering methods to suppress the impact of SEPs on TEPs. We found that, despite SEPs being lower in amplitude than TEPs induced by the same stimulation intensities, the two conditions were highly correlated in both space and time after ~60 ms, suggesting that sensory input accounts for some of the spatiotemporal characteristics of TEPs. Among the three filtering methods tested to suppress SEPs in TEP recordings, SSP-SIR showed a good trade-off between preserving the early responses while correcting the highly affected late components. Removing SEPs from TEPs revealed that even the late deflections in TEPs could not be fully explained by sensory inputs, suggesting TEPs at least partly reflect the cortical response to TMS. Changing the stimulation parameters (i.e.

intensity and waveform) resulted in similar TEP-SEP correlations across time and space, and similar performance of SEP suppression methods.

Similarities and differences between TEPs and SEPs

The N100 is perhaps the most extensively investigated peak in TMS-EEG recordings [10, 20, 35-38] and is thought to reflect cortical inhibition in both the motor and prefrontal cortices [7, 38]. However, an N100 peak is frequently observed following a variety of sensory stimuli, including auditory [19, 39], somatosensory [19, 40], visual [41], pain [42] and olfactory [43] stimuli. Accordingly, an N100-P180 complex is observed following TMS pulses without cortical stimulation, resulting from the loud TMS click (air-conducted auditory component) and coil vibration (bone-conducted auditory and somatosensory component) [18, 44, 45]. As a result, it is common practice to apply noise masking through headphones and a layer of foam between the scalp and coil to mitigate these sensory inputs during TMS-EEG recordings [12, 19]. Despite applying these masking methods, we found considerable similarities between EEG responses to cortical and shoulder stimulation across different TMS intensities and pulse shapes. The observed relationship suggests that TEPs following motor cortex stimulation contain some potentials unrelated to the direct cortical responses to TMS, especially at later components (e.g. N100, P180 and N280).

Despite the similarities between conditions, the differences observed in the scalp pattern and amplitudes between cortical and shoulder responses imply that TEPs following motor cortex TMS cannot be entirely explained by SEPs. In particular, early TEPs (<60 ms) were not significantly correlated with shoulder SEPs, and a cluster of electrodes over the site of stimulation remained independent of SEPs even at later

intervals including the N100 and P180 peaks. These results suggest that TEPs contain a combination of signals reflecting TMS-evoked and sensory-evoked potentials. While it is likely that this residual signal reflects the cortical response to TMS, we cannot rule out a contribution of other types of sensory inputs triggered by TMS not controlled for by shoulder stimulation, such as the contraction of cranial muscles or re-afferent sensory input from MEPs.

Our findings are comparable to two recent studies which also showed similarities and differences between a realistic TMS control condition (electrical stimulation of the scalp including an auditory TMS click) and TMS to the motor [21], frontal or parietal cortex [20]. Importantly, the spatiotemporal pattern observed following shoulder stimulation in this study closely resembled the responses to the realistic control stimulations using electrical scalp stimulation, implying the induction of similar sensory potentials between control methods. However, stimulating the shoulder cannot match the sensations perceived by scalp stimulations somatotopically [20, 21, 46], and therefore the relationship between TEPs and SEPs may be underestimated in our study. Taken together, our findings add to a growing body of evidence that some, but not all, of the TEP response results from sensory input. The contribution of SEPs to TEPs underlines the necessity for carefully designed control conditions in TMS-EEG experiments, especially when one wants to draw inference about TMS-evoked cortical activity.

Suppressing SEPs in TEP recordings

Given that online masking methods do not completely prevent contamination of TEPs by SEPs, we compared three offline methods for suppressing SEP activity: ICA, linear

regression, and SSP-SIR. A major limitation in comparing these methods is the lack of a ground truth to benchmark performance against. Therefore, we evaluated each method based on the ability to correct later peaks with the focus on fronto-central regions, which were heavily contaminated by SEPs, without altering early signals especially around the site of stimulation, which were not as contaminated. Linear regression did not sufficiently reduce sensory contamination at later time periods. ICA was found to be more aggressive, strongly dampening the potentials (Fig. 3) and, more importantly, distorting the short latency peaks recorded around the site of stimulation (Fig. 5) [47]. Despite causing a substantial amplitude decrease, SSP-SIR showed a good trade-off between correcting the late and highly contaminated fronto-central potentials (Fig. 3, 5), while preserving the early potentials recorded at the least affected regions (Fig. 5, 6). Importantly, source estimation analysis following SSP-SIR correction were largely confined to the site of stimulation (M1), and to cortical areas that are strongly connected to M1, including ipsilateral supplementary motor area, ipsilateral premotor cortex, and contralateral M1, showing minimal overlaps with regions activated by shoulder stimulation (Fig. 4).

Separating two signals which are time-locked to the same event is an extremely challenging task, which relies on several assumptions. For instance, ICA assumes temporal independences of the underlying sources, an assumption which may not hold for time-locked signals such as TEPs and could explain why ICA removed so much of the signal. SSP-SIR also substantially attenuated the TEPs voltages. This could be due either to the high contamination of the TEPs with SEPs or because of high spatial-correlations between SEPs and the genuine TMS-evoked topographies, leading SSP-SIR to overcorrect the signals of interest. Although the amplitude of the residual

signals following SSP-SIR were below the range of TEPs frequently observed in the literature [10, 11, 22, 28, 35, 48], the potentials remained above baseline and the topographies were consistent with motor cortex activation. Another key assumption which underlies all three suppression methods is the assumption of linear superposition of the sensory-evoked and TMS-evoked cortical activity. For this assumption to hold, the networks activated by sensory and TMS input would need to be completely independent, which is difficult to test quantitatively. As such, the suppression methods tested in this paper may not be appropriate for stimulation sites which overlap with sensory networks. The next step in validating offline methods will be to assess the reliability and replicability of SEP suppression following stimulation of other brain areas.

Conclusion

In conclusion, we have shown similarities between the cortical responses to TMS over M1 and the shoulder, especially from ~60 ms following stimulation. The results imply that current practices for minimising auditory and somatosensory inputs during TMS do not completely eliminate the contribution of sensory inputs to TEPs from motor cortex and highlight the need for control conditions to detect and minimize these signals. However, TEPs could not be entirely explained by SEPs, either at early or late time points, implying that TEPs do contain signals reflecting the direct cortical responses to stimulation. Offline methods for suppressing sensory-evoked activity show promise for isolating TMS-evoked neural activity and will likely form an important step in obtaining cleaner and more reliable TEPs.

Acknowledgments

This research was supported by the National Health and Research Council of Australia (1072057, NR; 1104580, AF, NR) and the Australian Research Council (180100741, NR). The authors would like to thank Dr. Jaakko Nieminen and Dr. Ben D. Fulcher for valuable advice on data analysis.

Conflicts of interest

The authors declare no conflicts of interest.

References

[1] Ferreri F, Rossini PM. TMS and TMS-EEG techniques in the study of the excitability, connectivity, and plasticity of the human motor cortex. Reviews in the Neurosciences 2013;24(4):431-42.
[2] Chang J-Y, Fecchio M, Pigorini A, Massimini M, Tononi G, Van Veen BD. Assessing Recurrent Interactions in Cortical Networks: Modeling EEG Response to Transcranial Magnetic Stimulation. Journal of neuroscience methods 2018.
[3] Ilmoniemi RJ, Virtanen J, Ruohonen J, Karhu J, Aronen HJ, Näätänen R, et al. Neuronal responses to magnetic stimulation reveal cortical reactivity and connectivity. Neuroreport 1997;8(16):3537-40.
[4] Rosanova M, Casarotto S, Pigorini A, Canali P, Casali AG, Massimini M. Combining transcranial magnetic stimulation with electroencephalography to study human cortical excitability and effective connectivity. Neuronal Network Analysis: Springer; 2011, p. 435-57.
[5] Darmani G, Zipser CM, Böhmer GM, Deschet K, Müller-Dahlhaus F, Belardinelli P, et al. Effects of the selective α5-GABAAR antagonist S44819 on excitability in the human brain: a TMS–EMG and TMS–EEG phase I study. Journal of Neuroscience 2016;36(49):12312-20.
[6] Manganotti P, Acler M, Masiero S, Del Felice A. TMS-evoked N100 responses as a prognostic factor in acute stroke. Functional neurology 2015;30(2):125.
[7] Premoli I, Castellanos N, Rivolta D, Belardinelli P, Bajo R, Zipser C, et al. TMS-EEG signatures of GABAergic neurotransmission in the human cortex. Journal of Neuroscience 2014;34(16):5603-12.
[8] Nakazawa K, Zsiros V, Jiang Z, Nakao K, Kolata S, Zhang S, et al. GABAergic interneuron origin of schizophrenia pathophysiology. Neuropharmacology 2012;62(3):1574-83.
[9] Treiman DM. GABAergic mechanisms in epilepsy. Epilepsia 2001;42:8-12.
[10] Du X, Choa F-S, Summerfelt A, Rowland LM, Chiappelli J, Kochunov P, et al. N100 as a generic cortical electrophysiological marker based on decomposition of TMS-evoked potentials across five anatomic locations. Experimental brain research 2017;235(1):69-81.
[11] Rogasch NC, Fitzgerald PB. Assessing cortical network properties using TMS–EEG. Human brain mapping 2013;34(7):1652-69.
[12] Ilmoniemi RJ, Hernandez-Pavon JC, Mäkelä NN, Metsomaa J, Mutanen TP, Stenroos M, et al. Dealing with artifacts in TMS-evoked EEG. *Engineering in Medicine and Biology Society (EMBC), 2015 37th Annual International Conference of the IEEE.* IEEE; 2015:230-3.
[13] Ilmoniemi RJ, Kičić D. Methodology for combined TMS and EEG. Brain topography 2010;22(4):233.
[14] Mutanen TP, Kukkonen M, Nieminen JO, Stenroos M, Sarvas J, Ilmoniemi RJ. Recovering TMS-evoked EEG responses masked by muscle artifacts. Neuroimage 2016;139:157-66.
[15] Rogasch NC, Thomson RH, Farzan F, Fitzgibbon BM, Bailey NW, Hernandez-Pavon JC, et al. Removing artefacts from TMS-EEG recordings using independent component analysis: importance for assessing prefrontal and motor cortex network properties. Neuroimage 2014;101:425-39.

[16] Paus T, Sipila P, Strafella A. Synchronization of neuronal activity in the human primary motor cortex by transcranial magnetic stimulation: an EEG study. Journal of Neurophysiology 2001;86(4):1983-90.
[17] Massimini M, Ferrarelli F, Huber R, Esser SK, Singh H, Tononi G. Breakdown of cortical effective connectivity during sleep. Science 2005;309(5744):2228-32.
[18] Nikouline V, Ruohonen J, Ilmoniemi RJ. The role of the coil click in TMS assessed with simultaneous EEG. Clinical Neurophysiology 1999;110(8):1325-8.
[19] Ter Braack EM, de Vos CC, van Putten MJ. Masking the auditory evoked potential in TMS–EEG: a comparison of various methods. Brain topography 2015;28(3):520-8.
[20] Conde V, Tomasevic L, Akopian I, Stanek K, Saturnino GB, Thielscher A, et al. The non-transcranial TMS-evoked potential is an inherent source of ambiguity in TMS-EEG studies. NeuroImage 2018.
[21] Gordon PC, Desideri D, Belardinelli P, Zrenner C, Ziemann U. Comparison of cortical EEG responses to realistic sham versus real TMS of human motor cortex. Brain Stimulation 2018.
[22] Herring JD, Thut G, Jensen O, Bergmann TO. Attention modulates TMS-locked alpha oscillations in the visual cortex. Journal of Neuroscience 2015;35(43):14435-47.
[23] Verleger R, Kuniecki M, Möller F, Fritzmannova M, Siebner HR. On how the motor cortices resolve an inter-hemispheric response conflict: An event-related EEG potential-guided TMS study of the flankers task. European Journal of Neuroscience 2009;30(2):318-26.
[24] Rossi S, Hallett M, Rossini PM, Pascual-Leone A, Group SoTC. Safety, ethical considerations, and application guidelines for the use of transcranial magnetic stimulation in clinical practice and research. Clinical neurophysiology 2009;120(12):2008-39.
[25] Rossini PM, Burke D, Chen R, Cohen L, Daskalakis Z, Di Iorio R, et al. Non-invasive electrical and magnetic stimulation of the brain, spinal cord, roots and peripheral nerves: basic principles and procedures for routine clinical and research application. An updated report from an IFCN Committee. Clinical Neurophysiology 2015;126(6):1071-107.
[26] Rothwell J, Hallett M, Berardelli A, Eisen A, Rossini P, Paulus W. Magnetic stimulation: motor evoked potentials. Electroencephalogr Clin Neurophysiol Suppl 1999;52:97-103.
[27] Delorme A, Makeig S. EEGLAB: an open source toolbox for analysis of single-trial EEG dynamics including independent component analysis. Journal of neuroscience methods 2004;134(1):9-21.
[28] Rogasch NC, Sullivan C, Thomson RH, Rose NS, Bailey NW, Fitzgerald PB, et al. Analysing concurrent transcranial magnetic stimulation and electroencephalographic data: a review and introduction to the open-source TESA software. Neuroimage 2017;147:934-51.
[29] Tadel F, Baillet S, Mosher JC, Pantazis D, Leahy RM. Brainstorm: a user-friendly application for MEG/EEG analysis. Computational intelligence and neuroscience 2011;2011:8.
[30] Hyvärinen A, Oja E. Independent component analysis: algorithms and applications. Neural networks 2000;13(4-5):411-30.
[31] Oostenveld R, Fries P, Maris E, Schoffelen J-M. FieldTrip: open source software for advanced analysis of MEG, EEG, and invasive electrophysiological data. Computational intelligence and neuroscience 2011;2011:1.

[32] Charter RA, Larsen BS. Fisher's z to r. Educational and Psychological Measurement 1983;43(1):41-2.
[33] Dunn OJ, Clark V. Correlation coefficients measured on the same individuals. Journal of the American Statistical Association 1969;64(325):366-77.
[34] Blair RC, Karniski W. An alternative method for significance testing of waveform difference potentials. Psychophysiology 1993;30(5):518-24.
[35] Casula E, Rocchi L, Hannah R, Rothwell J. Effects of pulse width, waveform and current direction in the cortex: A combined cTMS-EEG study. Brain stimulation 2018.
[36] Johnson JS, Kundu B, Casali AG, Postle BR. Task-dependent changes in cortical excitability and effective connectivity: a combined TMS-EEG study. Journal of neurophysiology 2012;107(9):2383-92.
[37] Kaarre O, Äikiä M, Kallioniemi E, Könönen M, Kekkonen V, Heikkinen N, et al. Association of the N100 TMS-evoked potential with attentional processes: A motor cortex TMS–EEG study. Brain and cognition 2018;122:9-16.
[38] Rogasch NC, Daskalakis ZJ, Fitzgerald PB. Cortical inhibition of distinct mechanisms in the dorsolateral prefrontal cortex is related to working memory performance: a TMS–EEG study. Cortex 2015;64:68-77.
[39] Scherg M, Vajsar J, Picton TW. A source analysis of the late human auditory evoked potentials. Journal of Cognitive Neuroscience 1989;1(4):336-55.
[40] Wang AL, Mouraux A, Liang M, Iannetti GD. The enhancement of the N1 wave elicited by sensory stimuli presented at very short inter-stimulus intervals is a general feature across sensory systems. PloS one 2008;3(12):e3929.
[41] Mangun GR, Hillyard SA. Modulations of sensory-evoked brain potentials indicate changes in perceptual processing during visual-spatial priming. Journal of Experimental Psychology: Human perception and performance 1991;17(4):1057.
[42] Greffrath W, Baumgärtner U, Treede R-D. Peripheral and central components of habituation of heat pain perception and evoked potentials in humans. Pain 2007;132(3):301-11.
[43] Pause BM, Sojka B, Krauel K, Ferstl R. The nature of the late positive complex within the olfactory event-related potential (OERP). Psychophysiology 1996;33(4):376-84.
[44] Nikulin VV, Kičić D, Kähkönen S, Ilmoniemi RJ. Modulation of electroencephalographic responses to transcranial magnetic stimulation: evidence for changes in cortical excitability related to movement. European Journal of Neuroscience 2003;18(5):1206-12.
[45] Tiitinen H, Virtanen J, Ilmoniemi RJ, Kamppuri J, Ollikainen M, Ruohonen J, et al. Separation of contamination caused by coil clicks from responses elicited by transcranial magnetic stimulation. Clinical neurophysiology 1999;110(5):982-5.
[46] Allison T, McCarthy G, Wood CC. The relationship between human long-latency somatosensory evoked potentials recorded from the cortical surface and from the scalp. Electroencephalography and Clinical Neurophysiology/Evoked Potentials Section 1992;84(4):301-14.
[47] Li R, Principe JC. Blinking artifact removal in cognitive EEG data using ICA. *Engineering in Medicine and Biology Society, 2006. EMBS'06. 28th Annual International Conference of the IEEE.* IEEE; 2006:5273-6.
[48] Komssi S, Aronen HJ, Huttunen J, Kesäniemi M, Soinne L, Nikouline VV, et al. Ipsi-and contralateral EEG reactions to transcranial magnetic stimulation. Clinical Neurophysiology 2002;113(2):175-84.